Estimating system OSNR with a digital coherent transceiver

Rongqing Hui, Charles Laperle, Doug Charlton, and Maurice O'Sullivan

Abstract—We demonstrate a technique of evaluating optical signal to noise ratio (OSNR) associated with an optical carrier in a fiber-optic system using a commercial coherent optical transceiver equipped with digital signal processing capability. The procedure of measuring noises caused by the transmitter and the receiver is outlined, and these transceiver-related noises need to be taken into account in order to accurately evaluate the system OSNR. Through digital polarization-demultiplexing and polarization nulling in the receiver, it is possible to extract the noise underneath the optical signal, and to measure the tilt of the ASE noise spectrum within the optical signal bandwidth.

Index Terms— Optical communication, coherent optical system, optical system performance monitoring, optical signal to noise ratio, optical transceiver, optical telemetry, fiber-optics

I. INTRODUCTION

Optical signal to noise ratio (OSNR) is one of the most important parameters of an optical system affecting the transmission performance [1]. In recent years polarizationmultiplexed (PM) coherent transceivers (modems) with digital signal processing (DSP) capabilities have been widely adopted for high speed fiber-optic transmission, which are highly flexible in terms of arbitrary waveform generation in the transmitter (Tx) and signal analysis at the receiver (Rx) all in the digital domain [2-4]. Coherent transceivers have been used for the estimation of system OSNR caused by both linear and nonlinear noise contributions. Most of these techniques [5-7] based on the recovery of transmitted data symbols do not consider transceiver-originated noise, which may impact the measurement accuracy at high OSNR levels. Some recent works [8,9] considered the impact of transceiver noise in OSNR monitoring based on neural network training, but the impacts of Tx and Rx cannot be separated. For open optical networks [10,11] composed of equipment from multiple vendors, the procedure of identifying performance impairments caused by individual equipment such as Tx, Rx, and in-line erbium-doped optical amplifiers (EDFAs) is of particular importance to performance optimization and troubleshooting.

In this paper we present a technique to measure system OSNR utilizing a commercial PM-coherent transceiver. A procedure is outlined to measure the noise contributions from

the Tx and the Rx independently, and remove these when evaluating the delivered OSNR. By measuring a time-gated complex waveform in the Rx, we show that the optical noise spectrum within the signal bandwidth can be measured including the tilt of the noise spectrum. The method of estimating modem noise is demonstrated here in the absence of Kerr nonlinear noise (KNN) but is not exclusive of this case. The estimate of OSNR, would require an associated estimate of KNN as in [5,8,9,12], otherwise it provides the OSNR equivalent of noise adduced in propagation, sometimes referred to as generalized optical signal to noise ratio (GOSNR) [13].

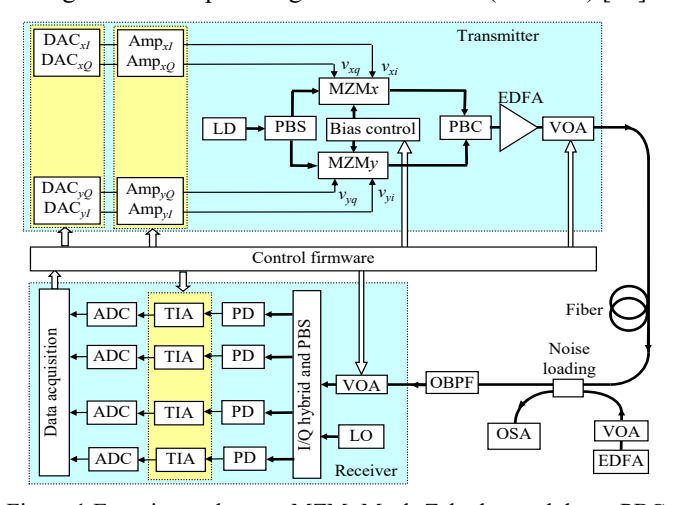


Figure 1 Experimental setup. MZM: Mach-Zehnder modulator, PBC: polarization combiner, PBS polarization splitter, OBPF: optical bandpass filter, VOA: variable optical attenuator, TIA: transimpedance amplifier

II. EXPERIMENTAL SETUP AND PROCEDURE

In this work, a commercial PM-coherent optical transceiver (Ciena WaveLogic Ai) is used to demonstrate the proposed technique. Fig. 1 shows the experimental setup in which the general structure of the transceiver is described. The Tx is equipped with two in-phase(I)/quadrature(Q) modulators to perform independent complex modulation of x- and y-polarized optical fields emitting from the same tunable laser diode (LD). The real and imaginary parts of a complex waveform can be designed and applied to each modulator through two digital-to-analog converters (DAC), and driving amplifiers with >34GHz

This work was supported in part by the US National Science Foundation under Grant CNS-1956137, and by Ciena Corporation.

R. Hui (e-mail: hui@ittc.ku.edu) is with the Department of Electrical Engineering and Computer Science, University of Kansas, Lawrence, KS 66045 USA. Maurice O'Sullivan (e-mail: mosulliv@ciena.com), Charles

Laperle (e-mail: claperle@ciena.com) and Doug Charlton (e-mail: dcharlto@ciena.com) are with Ciena Corporation, Ottawa, ON, K2K 0L1, Canada

analog bandwidth. The Rx detects signal complex optical field through an optical local oscillator (LO), a 90° hybrid, a polarization beam splitter, and 4 balanced, high speed photodiodes to produce photocurrents proportional to the I and Q components of x- and y-polarized optical channels. Each photocurrent signal is amplified by a trans-impedance amplifier (TIA) and digitized by an analog-to-digital converter (ADC). Both ADCs and DACs have 8-bit resolution. The digitized signal waveforms are then recorded for post-processing. Data input/output and operating conditions of both the Tx and the Rx are controlled through a firmware interface which can enable and disable various functional blocks. Optical noise loading is used in the fiber system to vary the level of system OSNR through an EDFA acting as a noise source and a variable optical attenuator (VOA) to change the level of added optical noise.

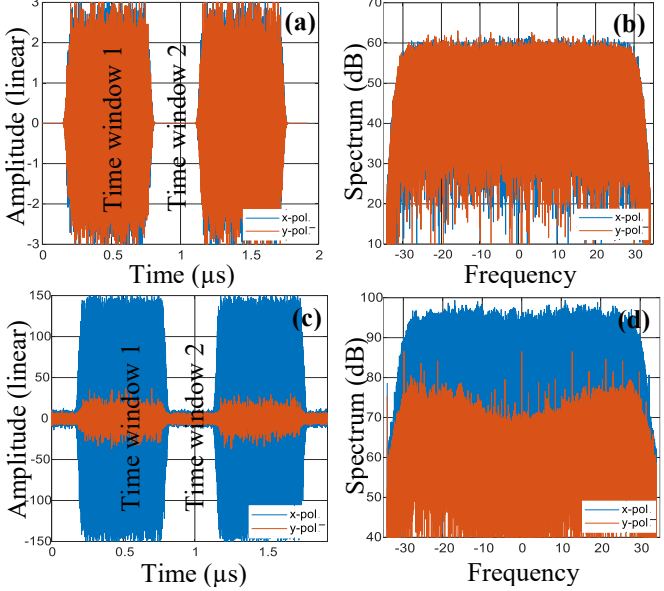


Figure 2. (a) and (b): amplitude and spectrum of x- and y-polarized waveforms loaded into the coherent Tx. (c) and (d): amplitude and spectrum of x- and y-polarized waveforms recovered in the coherent Rx when the Tx is loaded only with the x-polarized channel.

In order to measure the system OSNR accurately with the coherent transceiver, it is very important to remove noise contributions from both the Tx and Rx. Based on the transceiver block diagram shown in Fig. 1, major noise sources in the Tx include DAC digitizing noise, RF noise of amplifiers driving the modulators, and ASE noise generated by the EDFA post-amplifier inside Tx. Dominant noise sources of the Rx include shot noise mainly caused by the LO, amplification noise of the TIA, and digitizing noise of the ADC. Identifying individual noise contributions of Tx and Rx not only help characterizing transceiver performance, but are also necessary to obtain accurate OSNR of the system. The purpose of Tx waveform design and measurement procedure that will be described below is to isolate various noise contributions.

Time-gated complex data sequences of Gaussian statistics with a 30 GHz bandwidth shaped by a 10th order Super-Gaussian filter are loaded to the Tx. Both modulators are biased for maximum carrier suppression, which is the same as if they were used in normal operation. In time domain, as shown in Fig. 2(a) (only shows the real part), waveform exists only in time

window 1, and the amplitude is zero for time window 2. Fig. 2(b) shows the spectra of complex waveforms for the x- and y-polarized channels of the Tx.

In the experiment, we can selectively load one or both polarization channels to the Tx, and analyze waveforms detected by the Rx to extract system parameters. However, a commercial PM coherent Rx is designed to operate with polarization-multiplexed optical signals, and automatic gain control (AGC) of each TIA attempts to equalize the average signal voltages for all the 4 TIA outputs for optimum ADC performance. If the optical signal is single-polarized, the gain of the 4 TIAs would vary randomly with signal polarization, preventing the linear reconstruction of the complex optical field. With this Rx constraint in mind, our measurement procedure is outlined in the following 4 steps: (1) Load both xand y-polarized channels into the Tx so that the Rx can reach its nominal operation condition, and then disable all AGCs to freeze the TIA gain. (2) Turn off RF amplifiers which drive the modulator of the y-polarized channel so that the Tx output only has the x-polarized channel. (3) Record digital waveforms from all the 4 ADCs of the Rx for post-processing. In time window 2 the variance difference between x- and y-polarized channels represents the Tx noise caused by RF driving amplifiers and DACs. (4) Minimize signal optical power to the Rx by maximizing VOA attenuation (> 30dB), and measure signalindependent Rx noise, which includes LO-induced shot noise, thermal noise, TIA noise and ADC digitizing noise.

Due to fiber birefringence, polarization axes of the Tx and Rx need to be re-aligned to recover the complex optical fields of the *x*- and *y*-polarized channels in step (3) mentioned above. This can be accomplished with a Jones matrix operation [14],

$$\begin{bmatrix} E_x(f) \\ E_y(f) \end{bmatrix} = \begin{bmatrix} \cos \psi & -e^{-j\xi(f)} \sin \psi \\ e^{j\xi(f)} \sin \psi & \cos \psi \end{bmatrix} \begin{bmatrix} E_{x0}(f) \\ E_{y0}(f) \end{bmatrix}$$
(1)

where $E_{v0}(f)$ and $E_{v0}(f)$ are complex fields measured at the 4 ADCs in the Rx, and $E_x(f)$ and $E_y(f)$ are the recovered complex fields after removing the birefringence of the fiber. ψ represents polarization angle, and $\xi(f) = 2\pi f \delta t$ represents frequencydependent differential phase, with δt a differential group delay between the x- and y- polarization components [16]. As the Txonly emits the x-polarized channel, matrix parameters ψ and δt can be obtained by minimizing the power of $E_{\nu}(f)$ with a numerical search loop. Fig. 2 (c) shows the amplitudes of recovered waveforms E_x and E_y (only real parts) without optical noise loading. In time window 1, the power ratio between the x- and y-polarization components is about 20 dB. Whereas in time window 2, noise measured for the y-polarization is mainly caused by the Rx noise (y- channel is turned off in the Tx), but noise in the x-polarization includes both Tx noise and Rx noise. Fig. 2 (d) shows the power spectra of the recovered $E_x(f)$ and $E_{\nu}(f)$ where polarization extinction ratio can be higher than 25 dB in the low frequency region, but reduces to less than 18 dB in high frequency regions of beyond ±15 GHz. This reduced polarization extinction is attributed to the phase mismatch in I/Q reconstruction which is usually more noticeable at high frequencies, as well as the contribution of Rx noise which is independent of signal polarization. OSNR measurement based

on polarization diversity followed by direct detection can be susceptible to polarization mode dispersion (PMD) [15], but this does not apply for a PM coherent Rx which detects and reconstructs complex optical fields. In addition, as time-gated waveforms are used here, and noise is only measured in time window 2, polarization nulling only needs to minimize the Tx noise contribution in time window 2, which is already small.

III. RESULTS AND DISCUSSION

In order to demonstrate the proposed technique to work with a wide range of OSNR, variable optical noise loading is applied to the fiber system as shown in Fig. 1, and an OSA is used to monitor the OSNR for comparison with that measured by the digital Rx. The right y-axis of Fig. 3 shows the relative signal and noise powers measured from their variances scaled by the Rx responsivity, as the functions of system OSNR measured by the OSA. In the process of measuring OSNR by the Rx, signal power was obtained from the variance of the x-polarized waveform during time-window 1, and noise powers were obtained during time-window 2 for either x- or y-polarized components for comparison. Noise power of x-polarized component includes Tx noise in time-window 2 because the amplifiers driving the x-polarization modulator are powered-on even though the modulating signal is zero in that window. On the other hand, driving amplifiers of the y-polarized channel in the Tx are powered off, so that Tx noise is minimized. Although a small amount of optical carrier can leak through the ypolarization modulator if the bias control is not exactly at the null point, its impact can be removed by eliminating the very low frequency components (<10 MHz) when measuring the variance of the noise waveform. In the high OSNR region, xand y-polarized noise power levels can differ by as much as 4 dB because of the Tx noise contribution only exists in the xpolarized component which is stronger than the impact of optical noise in this region. This difference diminishes with the increase of optical noise and the decrease of OSNR, where the optical noise contribution becomes much stronger than the Tx noise in the low OSNR regime. The Rx noise floor, measured beforehand by blocking the optical signal into the Rx, is independent of the system OSNR, shown as a horizontal line in Fig. 3 (right y-axis).

Then the system OSNR with reference to 0.1nm noise bandwidth can be evaluated as,

$$OSNR_{0.1nm} = \frac{\sigma_{x-pol,T1}^2}{\sigma_{y-pol,T2}^2 - \sigma_{Rx}^2} \frac{F_{BW}}{12.5GHz}$$
 (2)

Where $\sigma_{x-pol,T1}^2$ is the variance (including signal and noise) in the x-polarization during time-window 1 with reference to Fig. 2(c), and $\sigma_{y-pol,T2}^2$ is the variance of the y-polarized noise during time-window 2 which does not include Tx noise. σ_{Rx}^2 is the variance of the Rx noise. A 10th order super-Gaussian digital filter with 30 GHz bandwidth is applied to all the received waveforms before measuring their variances for OSNR calculation, and thus the full noise bandwidth is $F_{BW} = 60$ GHz. The left y-axis of Fig. 3 shows the OSNR measured from the coherent Rx as the function of the OSNR measured by the OSA. Their agreement is within ± 0.5 dB except for the region of very high OSNR (>40 dB) where the accuracy requirement of Tx and

Rx noise estimation becomes more stringent as optical noise is very small in comparison. For the results presented in Fig. 3, each OSNR value is the average of 5 captured waveforms. The average Tx output and Rx input optical powers are -0.5dBm and -11 dBm, respectively. Note that the ASE contributed by the EDFA inside Tx is considered part of the accumulated system optical noise in the OSNR measurement. This is also the case when an OSA is used for the OSNR measurement.

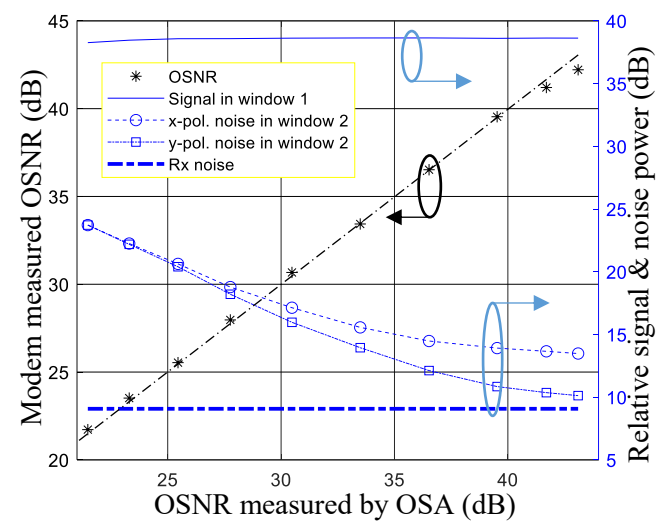


Figure 3. right y-axis: signal variance (thin solid line), x-polarized noise variance (open circles), y-polarized noise variance (open squares), and Rx noise variance (thick solid line) measured from the digital receiver as the function of OSNR measured by an OSA. Left y-axis: Stars: OSNR obtained from the digital receiver versus OSNR measured by OSA, dash-dotted straight line: linear fit of 1dB/1dB slope.

For OSNR estimation presented above, the spectrum of optical noise is uniform across the signal spectral window. However, in a practical optical system, the spectrum of accumulated ASE noise at the receiver may not always be flat, and the measurement of ASE noise spectral tilt underneath the signal spectrum can be quite challenging. One way to measure this ASE noise spectral tilt is to minimize the optical signal with a polarizer following a polarization controller [16]. As the optical signal is polarized (thus assuming only one polarization channel exists) and the optical noise is unpolarized, the polarizer can completely block the optical signal while only reducing the noise power spectral density by 3 dB. We show that a similar functionality can also be accomplished with a coherent optical receiver.

As an example, Fig. 4 shows the noise spectrum of the *y*-polarized component during time window 2 measured in step 3 and subtract the Rx noise spectrum obtained in step 4 of the procedure. As the Tx only sends the *x*-polarized channel which is needed to set the average optical signal power to maintain the normal operation of EDFAs in the transmission link, noise in the *y*-polarized component is primarily caused by the ASE noise of the system. The blue line in Fig. 4(a) is the noise spectrum measured by the coherent Rx. This was obtained with a flat optical noise spectrum loaded into the system, and the OSA trace is shown as the red line in the same figure for comparison. We then added an optical filter in the noise loading path to create a tilt in the optical noise spectrum shown in Fig. 4(b) as

the red line measured with an OSA. The corresponding noise spectrum measured by the coherent Rx shown as the blue line also shows the same tilt within the Rx bandwidth.

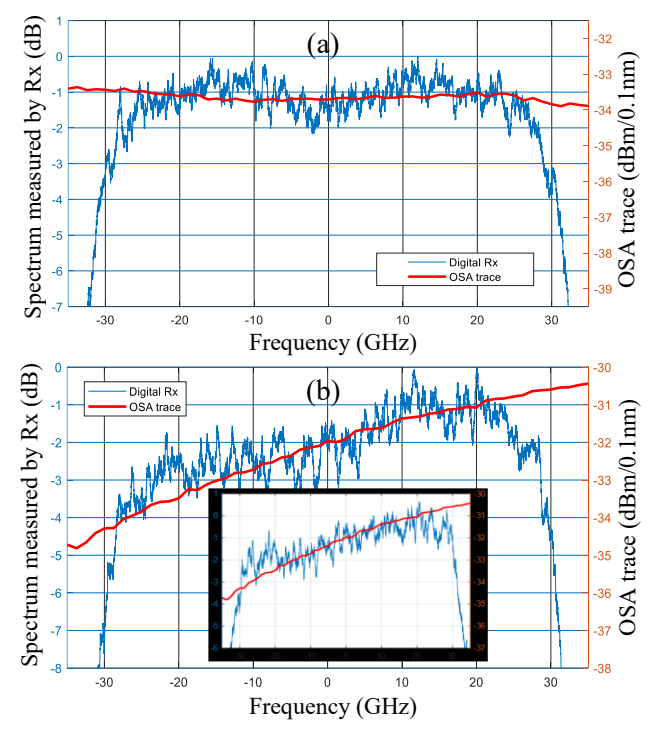


Figure 4. Comparison between normalized optical noise spectra measured with the digital coherent receiver (left y-axes), and optical noise spectra measured by an OSA (right y-axes) for the system with flat optical noise spectrum (a) and tilt optical noise spectrum (b). Inset in (b) (blue line) shows the tilt spectrum in (b) after subtracting the flat spectrum shown in (a) to remove Rx transfer function.

Note that OSNR measured with the coherent Rx shown in Fig. 3(b) is the power ratio between the signal and noise, which is independent of photodiode responsivity and TIA gain in the Rx. But the level of optical noise power spectral density (PSD) itself measured with the coherent Rx depends on the optoelectronic gain of the Rx. Thus, in Fig. 4 the noise PSD measured by the Rx are normalized only to indicate the spectral tilt of ASE noise. Although the detailed spectral shape of noise PSD measured by the coherent Rx can be affected to some extent by frequency response and gain equalization of photodetection and TIA circuits, Fig. 4 indicates a reasonably good agreement between the optical noise spectra measured by the coherent Rx and by an OSA. The noise spectral shape can be made more accurate if the transfer function of the Rx frontend can be separately characterized. For example, the noise spectrum measured with a flat ASE shown in Fig. 4(a) can be used as a reference for the calibration of Rx response. The blue curve in the inset of Fig. 4(b) shows the tilt spectrum of Fig. 4(b) after subtracting the Rx response to a flat ASE noise shown in Fig. 4(a).

As the proposed technique requires time-gated waveforms specially designed for system interrogation and noise detection, it is appropriate to be performed prior to actual data transmission to determine, for example, the maximum supported data rate based on linear channel quality, but not during data transmission.

IV. CONCLUSION

We have demonstrated a technique to evaluate OSNR in a fiber-optic system at the optical signal wavelength using a commercially available PM-coherent transceiver equipped with DSP capability. We show that the Tx and Rx noise can be strong enough to impact the accuracy of OSNR measurement. The procedure of measuring noises caused by the Tx and Rx, and removing them from OSNR estimation is outlined. Through digital polarization-demultiplexing and polarization nulling in the digital receiver, we have demonstrated that the shape of the optical noise spectrum underneath the signal can be measured, and the spectral tilt of the ASE noise across the optical signal bandwidth can be evaluated.

REFERENCES

- Z. Dong, F. N. Khan, Q. Sui, K. Zhong, C. Lu, and A. P. T. Lau, "Optical Performance Monitoring: A Review of Current and Future Technologies," J. Lightwave Technol., vol. 34, no. 2, pp. 525-543, 2016.
- [2] K. Roberts, Q. Zhuge, I. Monga, S. Gareau, and C. Laperle, "Beyond 100 Gb/s: Capacity, Flexibility, and Network Optimization", J. Optical Communications and Networking, vol. 9, no. 4, pp. C12-C24, 2017.
- [3] S. J. Savory, "Digital Coherent Optical Receivers: Algorithms and Subsystems," in IEEE Journal of Selected Topics in Quantum Electronics, vol. 16, no. 5, pp. 1164-1179, 2010.
- [4] H. J. Cho, S. Varughese, D. Lippiatt, R. Desalvo, S. Tibuleac, and S. E. Ralph, "Optical performance monitoring using digital coherent receivers and convolutional neural networks," Optics Express, vol. 28, no. pp. 32087-32104, 2020.
- [5] Z. Dong, A. Pak T. Lau, and C. Lu, "OSNR monitoring for QPSK and 16-QAM systems in presence of fiber nonlinearities for digital coherent receivers," Opt. Express vol. 20, pp. 19520-19534, 2012
- [6] X. Lin, O. A. Dobre, T. M. N. Ngatched, Y. A. Eldemerdash and C. Li, "Joint Modulation Classification and OSNR Estimation Enabled by Support Vector Machine," in IEEE Photonics Technology Letters, vol. 30, no. 24, pp. 2127-2130, 2018
- [7] M. S. Faruk, Y. Mori and K. Kikuchi, "In-Band Estimation of Optical Signal-to-Noise Ratio from Equalized Signals in Digital Coherent Receivers," in IEEE Photonics Journal, vol. 6, no. 1, pp. 1-9, 2014
- [8] A. D. Shiner, et al., "Neural Network Training for OSNR Estimation From Prototype to Product," Optical Fiber Communication Conference paper M4E.2, 2020
- [9] F. J. V. Caballero et al., "Machine learning based linear and nonlinear noise estimation," in IEEE/OSA Journal of Optical Communications and Networking, vol. 10, no. 10, pp. D42-D51, Oct. 2018
- [10]M. Filer, M. Cantono, A. Ferrari, G. Grammel, G. Galimberti, and V. Curri, "Multi-Vendor Experimental Validation of an Open Source QoT Estimator for Optical Networks," J. Lightwave Technol., vol. 36, no. 15, pp. 3037-3082, 2018.
- [11] J-L. Auge, V. Curri, E. L. Rouzic, "Open design for multi-vendor optical networks," Optical Fiber Communication Conference (OFC), paper Th11.2, 2019
- [12]F. Vacondio, O. Rival, C. Simonneau, E. Grellier, A. Bononi, L. Lorcy, J.-C. Antona, and S. Bigo, "On nonlinear distortions of highly dispersive optical coherent systems," Opt. Express vol. 20, no. 2, pp. 1022-1032, 2012.
- [13]D. Gariépy, S. Searcy, G. He, S. Tibuleac, M. Leclerc, and P. Gosselin-Badaroudine, "Novel OSNR Measurement Techniques Based on Optical Spectrum Analysis and Their Application to Coherent-Detection Systems," J. Lightwave Technol. 37, 562-570 (2019).
- [14] Fiber Optic Measurement Techniques, by R. Hui and M. O'Sullivan, Academic Press 2009
- [15]Q. Sui, A. P. T. Lau and C. Lu, "OSNR Monitoring in the Presence of First-Order PMD Using Polarization Diversity and DSP," in Journal of Lightwave Technology, vol. 28, no. 15, pp. 2105-2114, 2010
- [16]J. H. Lee, H. Y. Choi, S. K. Shin, and Y. C. Chung, "A Review of the Polarization-Nulling Technique for Monitoring Optical-Signal-to-Noise Ratio in Dynamic WDM Networks," J. Lightwave Technol., vol. 24, no. 11, pp. 4162-4171, 2006.